# Using scaling, fluctuation analysis to quantify natural and anthropogenic climate change

S. Lovejoy,
Physics, 3600 University st.,
Montreal, Que. H3A 2T8
Canada

## 1. Introduction

While current global warming certainly has a large anthropogenic component, its quantification relies primarily on complex GCM assumptions and codes; it is desirable to complement this with empirically based methodologies. Previous attempts to use the recent climate record have concentrated on "fingerprinting" [*Knutti et al.*, 2002] or otherwise comparing the record with GCM outputs [*Wigley et al.*, 1997]. By using $CO_2$ radiative forcings as a linear surrogate for all anthropogenic effects we estimate the total anthropogenic warming and effective climate sensitivity finding: $\Delta T_{anth}$ = 0.87±0.15 K, $\lambda_{2x,CO2,eff}$ = 3.08 ±0.95 K. These are close the IPPC 2007 (AR4) values $\Delta T_{anth}$ = 0.74±0.18 K and $\lambda_{2x,CO2}$ = 2 - 4.5 K (equilibrium climate sensitivity) and are independent of GCM models, radiative transfer calculations and emission histories. We, statistically formulate the hypothesis of warming through natural variability by using centennial scale probabilities of natural fluctuations estimated using scaling, fluctuation analysis on multiproxy data. We take into account two nonclassical statistical features - long range statistical dependencies and "fat tailed" probability distributions (both of which greatly amplify the probability of extremes). Even in the most unfavourable cases, we may reject the natural variability hypothesis at confidence levels > 99%.

In the recent epoch (here, since 1880) solar and volcanic forcings and changes in land use have had very little impact on GCM variabilities, the latter are apparently dominated by anthropogenic emissions (greenhouse gases and aerosols [*Lovejoy et al.*, 2012b], appendix figs. B1, B2). This is consistent with recent work showing that the main regional skill of GCM climate predictions is precisely in their ability to model the effects of emissions [*van Oldenborgh et al.*, 2012]. In addition, a comparison of the variability of various solar and volcanic reconstructions shows [*Lovejoy and Schertzer*, 2012a] that the recent period has statistically very similar solar forcings when compared to 1610-1900 and that over a wide range of scales, the volcanic forcings are factors 2 - 3 weaker than for the period 1500-1900 (appendix fig. B3). These forcings are thus unlikely to be relevant for explaining the recent warming.

## 2. A simple statistical hypothesis about the warming

If the anthropogenic forcing is strong enough, then a simple model may suffice:

$$T_{globe}(t) = T_{anth}(t) + \Delta T_{nat}(t) + \varepsilon(t) \qquad (1)$$

Where $T_{globe}$ is the measured mean global temperature anomaly, $T_{anth}$ is the (large) anthropogenic contribution, $\Delta T_{nat}$ is the (perturbation) natural variability and $\varepsilon$ is the measurement error. The latter can be estimated from the differences between the various observed global series and their means; it is nearly independent of scale [*Lovejoy et al.*, 2013] and sufficiently small ($\approx \pm 0.03$ K) that we ignore it.

Let us consider $T_{anth}$; it should be proportional to radiative forcings ($R_F$); denoting the total anthropogenic value by $R_{F,anth}$ we have: $T_{anth} = \lambda R_{F,anth}$ where $\lambda$ is the climate sensitivity. For $CO_2$, there is general agreement about its $R_F$:

$$R_{F,CO_2} = R_{F,2xCO_2} \log\left(\rho_{CO_2} / \rho_{CO_2,pre}\right); \quad R_{F,2xCO_2} = 3.7 W/m^2; \quad \rho_{CO_2,pre} = 277\, ppm \qquad (2)$$

where $R_{F,2xCO2}$ is for $CO_2$ doubling, the values are from AR4. As detailed in Methods, since 1880, the emissions of $CO_2$, other long lived Greenhouse Gases (GHG) and aerosols, are all functions of global economic activity, so that the simplest strategy is to consider $R_{F,CO2}$ to be a well-measured linear surrogate for $R_{F,anth}$; this avoids radiative transfer and GCM modeling - including the considerable uncertainties that still surround the aerosol effects (appendix fig. B9). Fig. 1 shows the resulting regression of $\log_2\left(\rho_{CO_2}(t)/\rho_{CO_2,pre}\right)$ against $T_{globe}(t)$; the result is indeed fairly linear with slope equal to the effective climate sensitivity to $CO_2$ doubling: $\lambda_{2x,CO2,eff}$ = 2.33±0.22 K (for 5 year averages for 1880-2004 and 1959-2004, the correlation coefficient is respectively $r$ = 0.38, 0.62). If desired, for the effects of a pure $CO_2$ doubling, we may use the proportionality constants 0.645 and 1.25 between $R_{F,anth}$ and $R_{F,CO2}$ (strong and weak aerosols, deduced from [*Myhre et al.*, 2001], [*Bauer and Menon*, 2012], see Methods): $\lambda_{2x,CO2,pure}$ = 3.61±0.34 and 1.86±0.18 K respectively.

It may be objected that the most immediate consequence of $R_F$ is to warm the oceans [*Lyman et al.*, 2010] so that we expect a time lag between the forcing and atmospheric warming (e.g. [*Hansen et al.*, 2005] finds a lag of 25- 50 years). By considering the time lagged cross correlation between $R_{F,CO2}$ and $T_{globe}$ it is found that at zero lag the cross-correlation reaches a value of ≈0.4 and stays fairly constant until lags of ≈ 20 years after which it quickly decreases (appendix fig. B4); the range 0 - 20 years brackets the significant range. If the above analysis is repeated with a 20 year lag, then the sensitivity increases to $\lambda_{2x,CO2,eff}$ = 3.82±0.54 K and slightly improves the statistics of the residuals, see below and appendix fig. B8. If we attribute the difference in the lagged and unlagged values

to random uncertainty, then we obtain the estimate $\lambda_{2x,CO2,eff}$ = 3.08 ±0.95 K. However, comparison with $CO_2$ data from Mauna Loa and the South Pole (since 1959) shows cross correlations decreasing after zero lag (appendix fig. B5) so that the relevance of using nonzero lags is unclear. All of the $\lambda_{2x,CO2,eff}$ estimates are comparable to others: e.g. 2- 4.5 K (AR4, see Methods). Our estimate has the advantage of being not only independent of GCM's, but also with respect to assumptions about radiative transfer, historical GHG and aerosol emission histories.

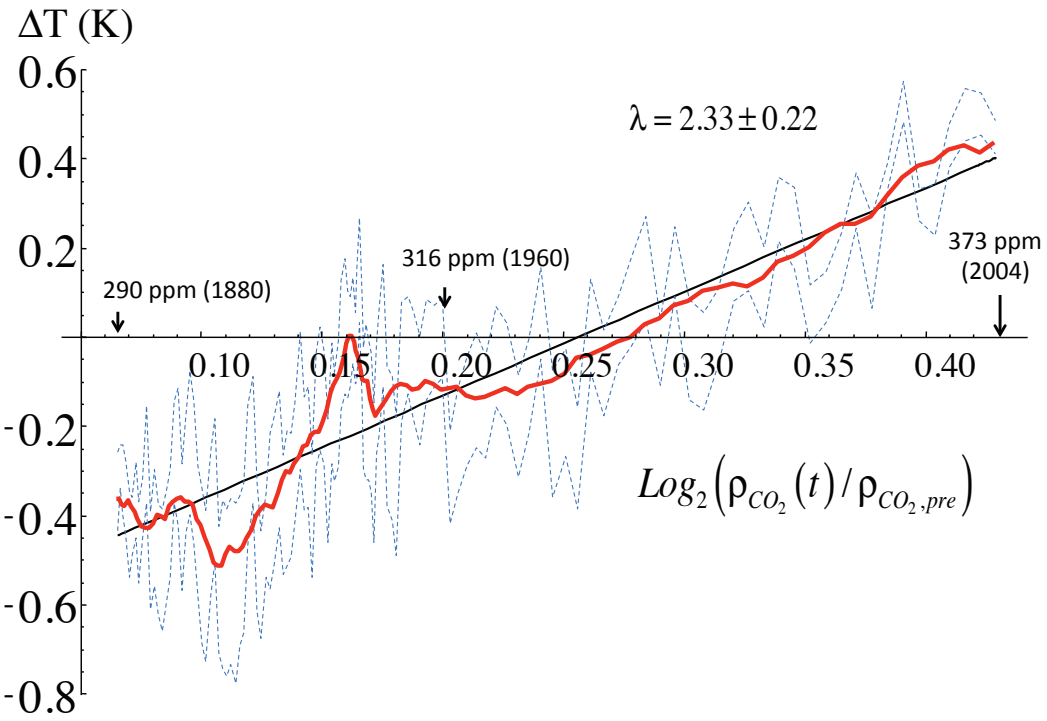


Fig. 1: The mean global temperature estimated from NASA-GISS, NOAA NCDC, HADCrut3 data bases as a functions of the logarithm of the mean $CO_2$ concentration from[*Frank et al.*, 2010]. The dashed lines represent the one standard deviation variations of the three series at one year resolution, the red line is the mean with a 10 year running average. Also shown is the linear regression with the effective climate sensitivity to $CO_2$ doubling: 2.33 ±0.22 K.

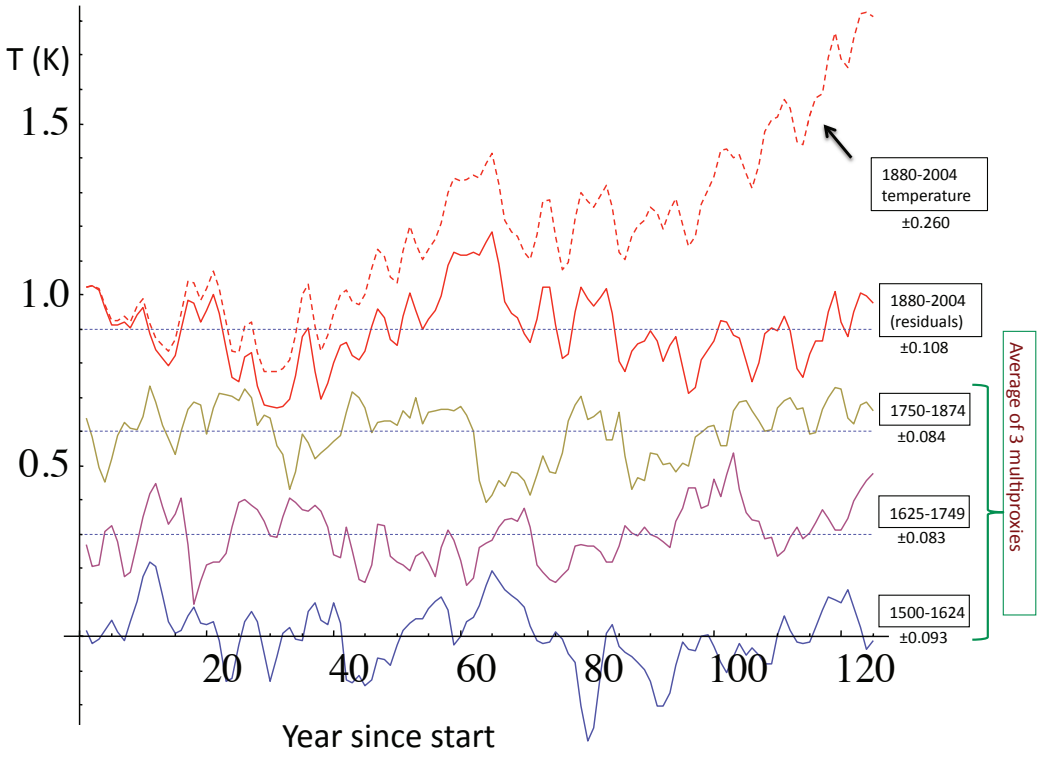


Fig. 2: The three lower curves are the means of the three multiproxies discussed in the text over three consecutive 125 year periods starting in the year 1500 with their standard deviations indicated. Each segment had its overall mean removed and was displaced by 0.3K in vertical for clarity. The fourth curve from the bottom is from the (unlagged) residuals with respect to the $CO_2$ regression in fig. 1 (1880-2004). The top curve is the annual resolution mean temperature. Whereas the curves from the three multiproxy epochs are quite similar to the residuals in the recent epoch, the actual recent epoch temperature shows a fairly systematic increase.

While the linearity of fig. 1 is encouraging (even impressive), its interpretation as representing an anthropogenic component is only credible if the residuals ($\Delta T_{nat}(t)$) have statistics very similar to those of $T_{globe}$ in pre-industrial epochs (where $T_{anth} = 0$) so that they could all be realizations of the same stochastic process. From fig. 2 - at the visual level – we see that the residuals are indeed comparable with similar preindustrial 125 year epochs (1500-1624, 16325-1749, 1750-1875) as estimated from three multiproxy series[*Huang*,

2004], [*Moberg et al.*, 2005], [*Ammann et al.*, 2007]. To make this similitude quantitative, in fig. 3 we consider the fluctuations as functions of time scale $\Delta t$ where fluctuations $\Delta T(\Delta t)$ are defined as the absolute differences in the means over the first and second halves of the interval $\Delta t$. This ("Haar") fluctuation has advantages over simply using the difference in temperature over the interval [*Lovejoy and Schertzer*, 2012b] (see Methods).

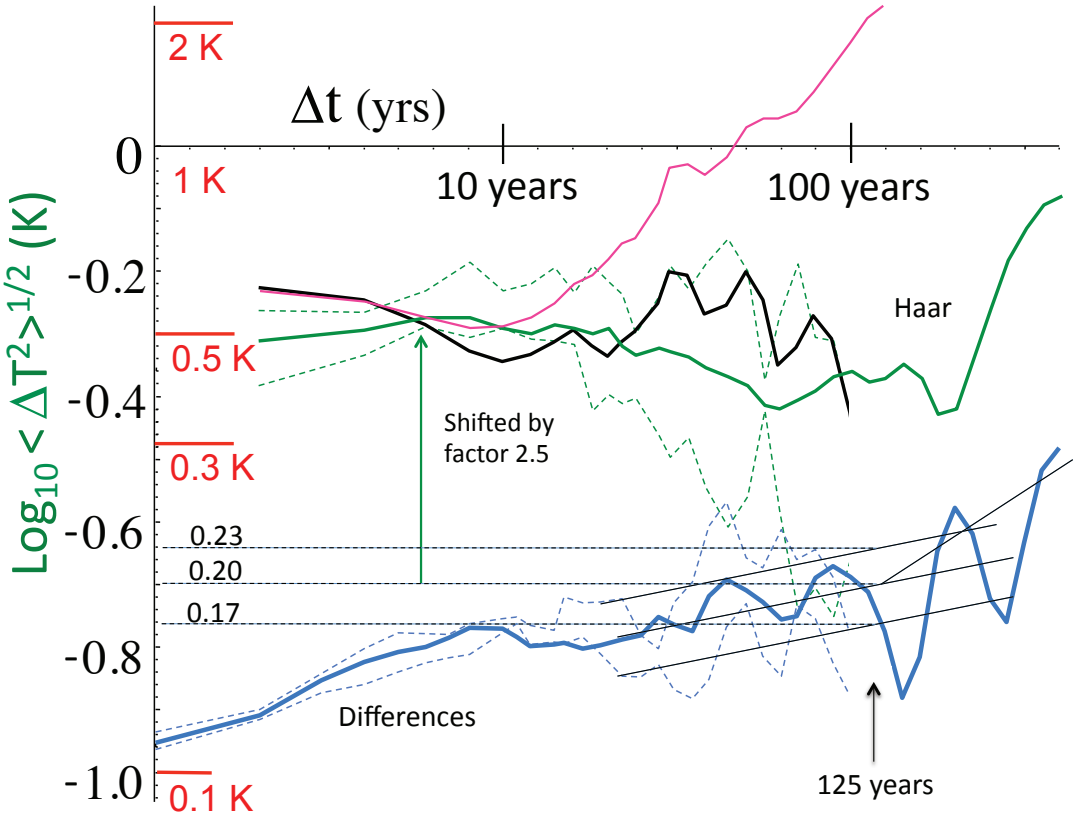


Fig. 3: The top (pink and green "Haar") curves show the RMS Haar fluctuations for the surface series (top, from [*Lovejoy and Schertzer*, 2012c]) and residuals (black) from 1880-2004 along with the corresponding curve for the multiproxies from 1500-1900 (long green curve) and one standard deviation error bars (dashed) estimated from the three 125 year epochs indicated in fig. 2. Over most of the range we see that the residuals are pretty much within the one standard deviation limits. The Haar fluctuations were multiplied by a "calibration" factor = 2 so that they would be close to

the difference fluctuations and then shifted upwards for clarity by a factor 2.5. Note that a straight line slope $H$ corresponds to a power law spectrum exponent $1+2H$ so that a flat line has spectrum $E(\omega) \approx \omega^{-1}$, and hence long range statistical dependencies (Gaussian white noise has slope -0.5). The roughly linear decline of the multiproxy variability to about $\Delta t \approx 100$ years is the (fluctuation cancelling) macroweather regime, the rise beyond it, the "wandering" climate regime [*Lovejoy*, 2013], [*Lovejoy and Schertzer*, 2013a].

The lower (blue) curves show the RMS difference fluctuations with one standard deviation limits (dashed) estimated from the epoch to epoch variability. The solid lines have slopes 0.15, 0.4 the former represent estimates of the mean and one standard deviation limits of the difference fluctuations. From the graph, at 125 years, this may be estimated as 0.20±0.03 K.

In figure 3, first note the comparison of the RMS fluctuations of the three surface series (1880-2008) with those of the three multiproxies (1500-1900). Up until $\Delta t \approx 10$ years they are quite close to each other (and slowly decreasing), then they rapidly diverge. However when we consider the RMS residuals we find they are mainly within the one standard deviation error bars of the epoch to epoch multiproxy variability so that removing the anthropogenic contribution gives residuals $\Delta T_{nat}$ with statistics close to those of the pre-industrial multiproxies (see also appendix fig. B7).

## 3. Estimating the probability that the warming is a consequence of natural variability

Regressing $R_{F,CO2}$ against the global mean temperature leads to satisfactory results in the sense that the residuals and preindustrial multiproxies are plausibly realizations of the same stochastic process. However, this result is not too sensitive to the exact method of estimating $T_{anth}$ and $\Delta T_{nat}$ - the 20 year lagged residuals are a bit better although using simply a linear regression of $T_{globe}$ against time is substantially worse; see appendix figs. B6, B8. From the point of view of determining the probability that the warming is natural, the key quantity is therefore the total anthropogenic warming $\Delta T_{ant} = T_{ant}(2004) - T_{ant}(1880)$.

Using the $\log_2\rho$ method (fig. 1) we find $\Delta T_{anth} \approx 0.85\pm0.08$ K and with a 20 year lag $\approx 0.90\pm0.13$ K. Treating the lag as a random uncertainty and combining the lagged and unlagged estimates, we obtain $\Delta T_{anth} \approx 0.87 \pm 0.15$; for comparison, for the linear in time method, we obtain $\approx 0.75\pm0.07$ K. We can also estimate an upper bound - the total range $\Delta T_{\text{globe,range}} = Max(\Delta T_{globe}) \approx 1.04\pm0.03$ K so that (presumably) $\Delta T_{\text{anth}} < \Delta T_{\text{globe,range}}$. Note that although in principle the probabilities could be estimated from the variability of multicentennial GCM variability in the pre-industrial epoch, these may be a bit too weak[*Lovejoy et al.*, 2012a] (see appendix figs. B1, B2).

We now estimate the probability distribution of $\Delta T$ from the multiproxies first over the shorter lags with reliable estimates of extremes (up to $\Delta t = 64$ years, fig. 4), and then using the scaling of the distributions and RMS fluctuations to deduce the form at $\Delta t = 125$ years, see Methods. We find the 125 year RMS temperature difference ($\left\langle \Delta T(125)^2 \right\rangle^{1/2} = \sigma_{125} = 0.20\pm0.03$ K. Since theoretically, scaling is associated with probabilities with power law "fat" tails (i.e. $Pr(\Delta T>s) \approx s^{-q_D}$ for the probability of a fluctuation exceeding a threshold $s$; $q_D$ is an exponent), in fig. 5 we compare $q_D = 4$, 6 and $q_D = \infty$ (a pure Gaussian). We see that the former two values bracket the distributions (including their extremes) over the whole range of large fluctuations (the extreme 3%).

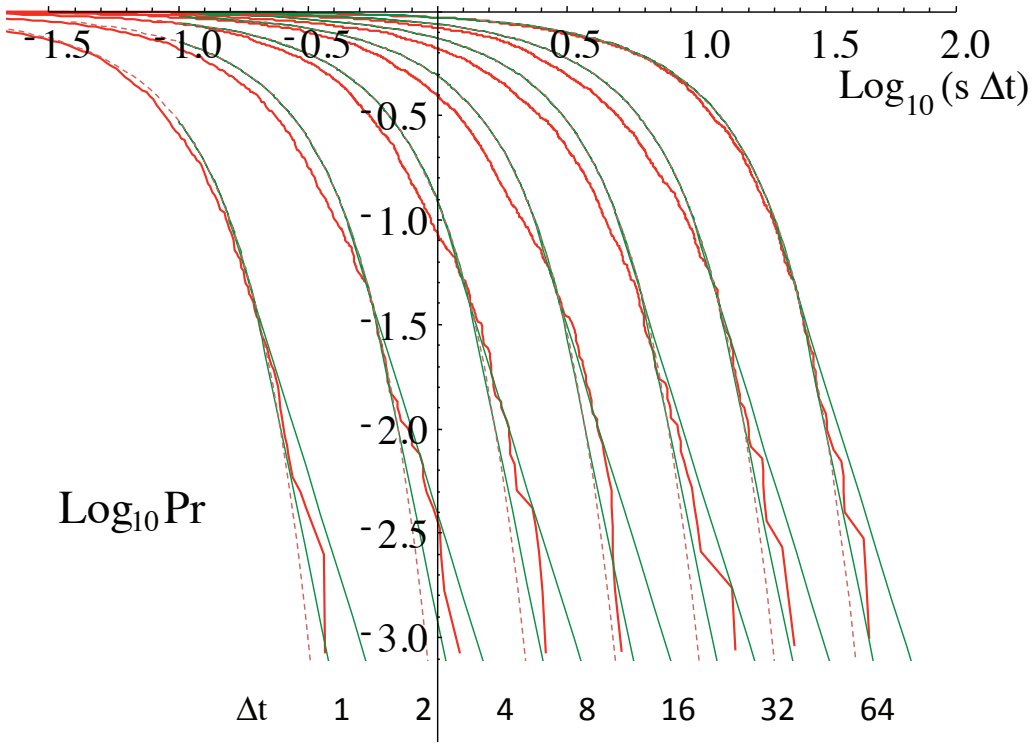


Fig. 4: This shows the total probability of random absolute temperature differences exceeding a threshold $s$ (in K). To avoid excessive overlapping, the latter were compensated by multiplying by the lag $\Delta t$ (in years, shifting the curves to right successively by $\log_{10}2 \approx 0.3$), the data are the pooled annual resolution multiproxies from 1500-1900. The reference curves are Gaussians with corresponding standard deviations (dashed) and with tails ($Pr \approx$<3%) corresponding to bounding $\Delta t^{-4}$ and $\Delta t^{-6}$ behaviours.

Stated succinctly, the statistical hypothesis on the natural variability is that its extreme probabilities ($Pr$ <3%) are bracketed by a modified Gaussian with $q_D$ between 4 and 6 and with standard deviation (and uncertainties) given by the scaling of the multiproxies in fig. 3: $\sigma_{125}$ = 0.20±0.03 K. With this, we can evaluate the corresponding probability bounds for various estimates of $\Delta T_{anth}$. These probabilities are conveniently displayed in fig. 5 by boxes. For example, the AR4 $\Delta T_{anth}$ = 0.74 ± 0.18 K (thick red box)

yields a probability ($p$): 0.009% < $p$ < 0.6% whereas the (unlagged) $\log_2\rho_{CO2}$ regression (filled red box) yields 0.0009% < $p$ < 0.2% and the 20 year lag (dashed blue) yields 0.002% < $p$ < 0.2%, with most likely values (using $q_D$ = 5) of 0.08%, 0.08%, 0.03% respectively. In even the most extreme cases, the hypothesis that the observed warming is due to natural variability may be rejected at confidence levels 1-$p$ >99%, and with the most likely values, at levels >99.9%. The other cases considered do not alter these conclusions (fig. 5).

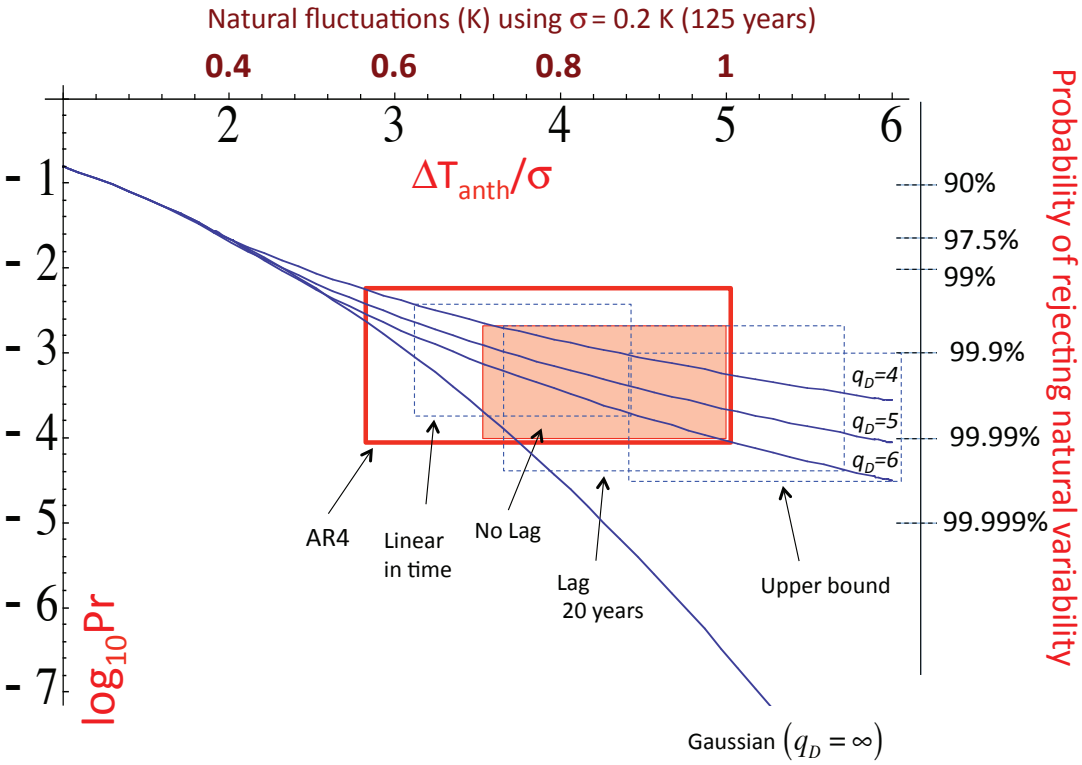


Fig. 5: The probability of anthropogenic warming by $\Delta T_{anth}$ as functions of the number of standard deviations for the five cases discussed in the text. Also shown for reference is the equivalent temperature fluctuation using the mean standard deviation at 125 years. The vertical sides of the boxes are defined by the one standard deviation limits of $\Delta T_{anth}$ /σ, the horizontal sides by the $q_D$ =4 (upper) and $q_D$ = 6 (lower) limits; the middle curve ($q_D$ = 5) is the mean (most likely) exponent. The classical statistical

hypothesis (Gaussian, corresponding to $q_D = \infty$) is indicated for reference. The AR4 GCM based values $\Delta T_{anth}$ =0.74 ± 0.18 are indicated by the thick red line and using $\log_2 \rho_{CO2}$ as a surrogate for the RF followed by linear regression ($\Delta T_{anth}$ =0.85 ± 0.08) is shown in the filled red box. The other cases are shown by dashed blue lines: $\log_2 \rho_{CO2}$ but with a 20 year lag, linear regression of $T_{globe}$ against time and the upper bound on $\Delta T_{anth}$ = 1.04±0.03.

## 5. Conclusions

Two aspects of anthropogenic global warming are frequent sources of frustration. The first is the lack of a quantitative theory of natural variability with which to compare the observed warming $\Delta T_{anth}$, the second is the near exclusive reliance on GCM's to estimate it. In this paper we have argued that since ≈ 1880, anthropogenic warming has dominated the natural variability to such an extent that straightforward empirical estimates of the total warming can be made. The one favoured here - using $CO_2$ $R_F$ as a surrogate for all anthropogenic $R_F$ - gives both effective sensitivities $\lambda_{2xCO2,eff}$ and total anthropogenic increases $\Delta T_{anth}$ (3.08±0.91 K and 0.87±0.15 K) comparable to the AR4 estimates (2 - 4.5 K and 0.74±0.18 K). The method was justified because we showed that over a wide range of scales, the residuals have nearly the same statistics as the preindustrial multiproxies. An additional advantage of this approach is that it is independent of many assumptions and uncertainties including radiative transfer, GCM and emission histories. The main uncertainty is whether or not to include a twenty year lag (included in the above estimates).

Whether one estimates $\Delta T_{anth}$ using the empirical method proposed here, or using a GCM based alternative, when $\Delta T_{anth}$ is combined with scaling properties of multiproxies we may estimate the probabilities as functions of time scale and test the hypothesis that the warming is due to natural variability. Our statistical hypothesis – supported by the multiproxy data - is that due to the scaling - there are long range

correlations in the temperature fluctuations coupled with nonclassical "fat tailed" probability distributions which bracket the observed probabilities. Both effects lead to significantly higher probabilities than would be expected from classical "scale bound" (exponentially decorrelated) processes and/or with "thin" (e.g. Gaussian or exponential) tails. However, even in the most extreme cases, we are still able to reject the natural variability hypothesis with confidence levels >99% - and with the most likely values - at levels >99.9%. Finally, fluctuation analysis shows that recent period solar forcing was close to preindustrial levels (at all scales), and that volcanic forcings were a factor 2-3 times weaker (at all scales), so that they cannot explain the warming either. While no amount of statistics will ever prove that the warming is indeed anthropogenic, it is nevertheless difficult to imagine an alternative.

## Appendix A: Methods

### A.1 Climate sensitivity

$\lambda_{2x,CO2,eff}$ is an "effective" sensitivity both because it uses $CO_2$ as a surrogate for all the anthropogenic $R_F$, and also because it is not a usual "equilibrium climate sensitivity" defined as "the equilibrium annual global mean temperature response to a doubling of equivalent atmospheric $CO_2$ from pre-industrial levels" (AR4). Since only GCM's can truly attain "equilibrium" (and this only asymptotically in a slow power law manner [*Lovejoy et al.*, 2013]), this climate sensitivity is really a theoretical / model concept that can at best only be approximated with real world data. Because of this difference in definition of climate sensitivity, it would be an exaggeration to claim that we have empirically validated the AR4 result, even though our value $\lambda_{2xCO2,eff} = 3.08 \pm 0.91$ (taking into account the

uncertainty in the lag) is very close to the AR4 value 2 - 4.5K (which itself is close to the AR1 – 3 value 3±1.5 K). It is not obvious whether effective or equilibrium sensitivities are more relevant for predicting the temperature rise in the 21st century.

**A.2 $CO_2$ as a linear surrogate for anthropogenic effects**

All the key anthropogenic effects are functions of economic activity and $CO_2$ levels are well measured and provide a convenient surrogate for the latter. Over the period 1880-2004, $\rho_{CO2}$ and $\log_2\rho_{CO2}$ are linear to within ±1.5% so that either $\rho_{CO2}$ or $R_{F,CO2}$ could be used. For example using data in [*Myhre et al.*, 2001] $R_{F,GHG}$ and $R_{F,CO2}$ are closely related and we find: $R_{F,GHG} = -0.190 \pm 0.019 + (1.793 \pm 0.027) R_{F,CO_2}$ with high correlation ($r_{CO2,GHG}$ = 0.945) so that $R_{F,CO2}$ may be considered "enhanced" by the other GHG by ≈ 79% (appendix fig. B9). Although ozone, biomass and other effects contribute, the main additional contribution – and uncertainty - in the total anthropogenic $R_{F,anth}$ is from the direct and indirect cooling effects of aerosols, and is still under debate. Recent estimates (for both effects) are ≈ -1.2 (AR4), -1.0 W/m$^2$, [*Myhre*, 2009] and ≈ -0.6 W/m$^2$, [*Bauer and Menon*, 2012] (all with large uncertainties). Using the Mauna Loa estimate for $\rho_{CO2}$ in 2012 (393.8 ppm, http://co2now.org/), these estimates can be compared to ≈ 1.9 W/m$^2$ for $CO_2$ and ≈ 3.1 W/m$^2$ for all GHG (the above relation). However, sulfate production [*Van Aardenne et al.*, 2001] (a surrogate for aerosols) is roughly linear with $R_{F,CO2}$ (over 1880-1990, we find $r$ = 0.60), so that whatever its $R_F$ effect – it is likely to also be roughly linear with $R_{F,CO2}$. This justifies the simple strategy adopted here of considering $R_{F,CO2}$ to be a well measured linear surrogate for $R_{F,anth}$; using the $R_{F,anth}$ data in [*Myhre et al.*, 2001] we obtain $R_{F,anth} = 0.034 \pm 0.033 + (0.645 \pm 0.048) R_{F,CO_2}$ with $r_{CO2,anth}$ = 0.852. This assumes -1.5 W/m$^2$ for aerosol cooling; if the most recent cooling estimates are correct (-0.6 W/m$^2$, i.e. they

are diminished by 60%), then we obtain a proportionality constant ≈ 1.25 rather than 0.645.

**A.3 Scaling fluctuation analysis**

The traditional way to characterize the variability over a wide range of scales is spectral analysis. It is typically found that climate spectra are dominated by red noise "backgrounds" and over wide ranges, these are roughly power laws (scaling) indicating that over the range, there is no characteristic scale and (in general) that there are long range statistical dependencies (e.g. correlations). However spectral analysis has disadvantages, the most important of which is that its interpretation is not as straightforward as real-space alternatives. This has lead to the development of wavelets and other methods of defining fluctuations (e.g. Detrended Fluctuation Analysis [*Peng et al.*, 1994]). However, [*Lovejoy and Schertzer*, 2012b] shows that the simple expedient of defining fluctuations over intervals $\Delta t$ by the differences in the means over the first and second halves of the interval ("Haar fluctuations") is particularly advantageous since unlike differences - which on (ensemble) average cannot decrease – Haar fluctuations can both increase and decrease with this critical distinction corresponding to a spectral exponent of $\beta = 1$ (ignoring small intermittency corrections). In regions where they increase they are proportional to differences, in regions where they decrease, they are proportional to averages so that the interpretation is very straightforward.

**A.4 The probability of extreme fluctuations over 125 year intervals**

To estimate the probability distribution of the extreme $\Delta T$ from the multiproxies, we first use fluctuation analysis – this time directly on differences (i.e. $\Delta T = T(t+\Delta t) - T(t)$) - to estimate the typical RMS 125 year temperature difference ($\left\langle \Delta T(125)^2 \right\rangle^{1/2} = \sigma_{125}$); see fig. 3.

Due to poor statistics at $\Delta t$ = 125 years there are large fluctuations, however, the use of scaling hypothesis (linearity on the log-log plot) allows us to estimate the mean of $\sigma_{125}$ with some confidence (see the reference lines). The uncertainty can also be estimated from the variability of the $\sigma_{125}$ over the three epochs, we obtain $\sigma_{125}$ = 0.20±0.03 K.

Since the RMS fluctuations are roughly scaling we expect that the probability distributions of $\Delta T$ for different $\Delta t$ will have a constant form. In addition, a generic result for scaling processes is that they have power law, "fat" probability tails. This is investigated in fig. 4 that shows the probability distribution of temperature differences $\Delta T$ for $\Delta t$ increasing by factors of 2 from 1 to 64 years. To obtain good statistics for the low probability, extreme $\Delta T$, all available $\Delta t$ intervals were used. However, when $\Delta t$ starts to approach the length of the series (here 400 years), then this effectively oversamples the relatively few large $\Delta t$ fluctuations, and underestimates the extremes, hence we did not go beyond 64 years. From the figure we see that the forms are indeed very similar and that they show clear evidence of excesses with respect to the Gaussian (dashed lines); indeed the observed probability excesses range from a factor 2.3 ($\Delta t$ =8) to 293 ($\Delta t$ = 16), with mean factor of 63. Similarly, fitting the extreme factor of 20 in probability to a power law (i.e. $Pr(\Delta T>s) \approx s^{-q_D}$), yields $q_D$ = 4.99±0.43. This is close to $q_D$ = 5 found in paleotemperature fluctuations at centennial and at millennial scales [*Lovejoy and Schertzer*, 1986], and at monthly and annual scales [*Lovejoy and Schertzer*, 2013b]. However, in order not to tie our conclusions to specific assumptions about the form of the tails, in fig. 4 we compared the actual distributions with those of Gaussians modified so that they smoothly asymptote to a power law with a given $q_D$. In the figure we therefore compare $q_D$ = 4, 6 and $q_D = \infty$ (a pure Gaussian); we see that the former two values bracket the distributions (including their extremes) over the whole range

of large fluctuations (the extreme ≈ 3%). Note that a more theoretically justified form of scaling probabilities is based on codimension functions[*Schertzer and Lovejoy*, 1987], but these generally have the same types of extreme (power law) behaviours and are unnecessary here.

# Appendix B: Data

### B.1 Instrumental data

We used globally, annually averaged temperature data over the period 1880 – 2008 from three sources: the NOAA NCDC (National Climatic Data Center) merged land, air and sea surface temperature dataset (abbreviated NOAA NCDC below), on a $5^o$x$5^o$ grid [*Smith et al.*, 2008], the NASA GISS (Goddard Institute for Space Studies) dataset [*Hansen et al.*, 2010] (from 1880 on a $2^o$x $2^o$) and the HadCRUT3 dataset [*Rayner et al.*, 2006] (on a $5^o$x$5^o$ grid). HadCRUT3 is a merged product created out of the HadSST2 Sea Surface Temperature (SST) dataset and its companion dataset of atmospheric temperatures over land, CRUTEM3 [*Brohan et al.*, 2006]. Both the NOAA NCDC and the NASA GISS data were taken from http://www.esrl. noaa.gov/psd/; the others from http://www.cru.uea. ac.uk/cru/data/temperature/. The NOAA NCDC and NASA GISS are both heavily based on the Global Historical Climatology Network [*Peterson and Vose*, 1997], and have many similarities including the use of sophisticated statistical methods to smooth and reduce noise. In contrast, the HadCRUT3 data are less processed, with corresponding advantages and disadvantages. Haar analysis of the space-time densities of the HadCRUT3 measurements shows that they are sparse in both space and time with fractal codimensions of ≈ 0.25, ≈0.2 respectively [*Lovejoy and Schertzer*, 2013b]. This strong sparseness means that we

should not be surprised that the resulting global series are somewhat dependent on the assumptions about missing data.

### B.2 Multiproxy data

Following the analysis in [*Lovejoy and Schertzer*, 2012c], the more recent (post 2003) multiproxies were argued to be more faithful to the low frequency (multicentennial) variability. In particular, the low frequencies in [*Huang*, 2004], [*Moberg et al.*, 2005] and [*Ljundqvist*, 2010] were found to be more realistic when compared to ice core paleotemperatures with fluctuations starting to increase in amplitude for $\Delta t \approx$>30 - 50 years (see fig. B1). However, one of these series (ref. [*Ljundqvist*, 2010]) was at 10 year resolution and was not suited for the present study which required annual series. It was therefore replaced by the Ammann et al series[*Ammann et al.*, 2007] which although having somewhat smaller multicentennial variability was statistically not too different (see e.g. fig. B7).

### B.3 Solar and volcanic reconstructions

In [*Lovejoy and Schertzer*, 2012a], a scaling fluctuation analysis was used to show that the two volcanic forcing reconstructions [*Crowley*, 2000], [*Gao et al.*, 2008] had fluctuations rapidly decreasing with scale $\Delta t$ and differing from each other mainly by a constant factor. It was therefore unlikely that they could account for multicentennial, multimillenial temperature fluctuations which increase with scale. Similarly, analysis of solar reconstructions found that they divided into two categories: the sunspot based reconstructions[*Lean*, 2000], [*Wang et al.*, 2005], [*Krivova et al.*,

2007] and the $^{10}$Be based reconstructions, [*Steinhilber et al.*, 2009], [*Shapiro et al.*, 2011] with the former having rapidly increasing fluctuations, and the latter, rapidly decreasing fluctuations. Within each group, the differences were mainly of amplitude (a constant factor). For the same reasons as the volcanic forcings are likely to be irrelevant at centennial and longer scales, if correct, the $^{10}$Be reconstructions would imply that solar forcings at these and longer scales are also irrelevant. Therefore, to judge possible changes in these forcings in the recent period, we only considered the more relevant sunspot based solar reconstructions, and this, only for the more reliable most recent two (fig. B3). We see that although they disagree with each other, there is practically no change at any scale when the recent epoch is compared to pre 1900 forcings so that we conclude that solar variability is statistically of the same type (stationary) over the relevant time periods. For the volcanic forcings, the recent epoch is consistently found to have weaker fluctuations at all scales, and this by a factor 2 -3 (fig. B3).

**B.4 The emissions**

The $CO_2$ emission data were taken from both Mauna Lao and South Pole stations (since 1959; used in fig. B5) and for the 1880-2004 $CO_2$ reconstruction, from [*Frank et al.*, 2010]. The long lived Greenhouse Gas (GHG) reconstruction as well as the total anthropogenic reconstruction (1880-1995) in fig. B9 were from [*Myhre et al.*, 2001] As indicted in the text (Methods), the main uncertainty in the latter is due to the role of aerosols. However, even if their contribution is diminished by a large fraction (perhaps

as much as 60% see the text), as long as this fraction is roughly constant over time, $R_{F,CO2}$ will remain a good surrogate for $R_{F,anth}$.

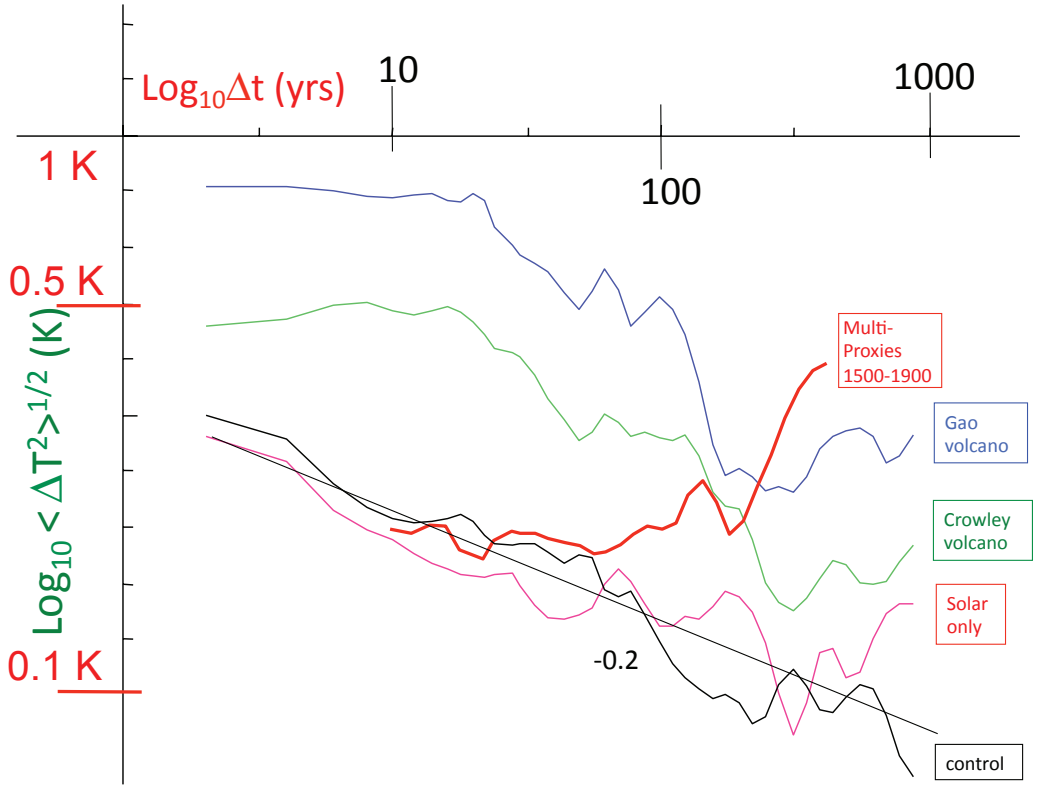


Fig. B1: This shows the RMS Haar fluctuations for the GISS-ER2 Last Millenium simulations for the period 1000-1900, annually averaged temperatures over land in the northern hemisphere. The control run shows the slow power law convergence ($\approx \Delta t^{-0.2}$) of the unforced model to its asymptotic climate state. The solar curve shows that putting solar forcings from reconstructed solar activity leads to similar low variability results. The two volcanic curves use different volcanic reconstructions [*Gao et al.*, 2008]. All of these are compared with the mean of three multiproxy reconstructions over the period 1500-1900 ([*Huang*, 2004], [*Moberg et al.*, 2005], [*Ljundqvist*, 2010]).

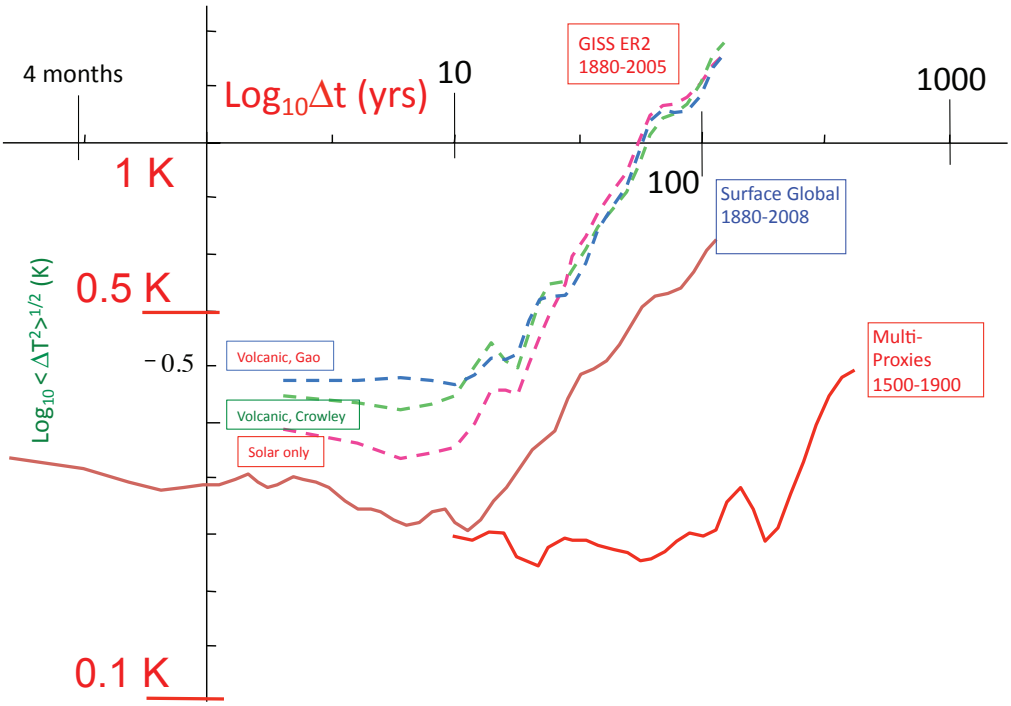


Fig. B2: This is the same as previous except for the period 1880-2005 (dashed) and compared to the mean RMS fluctuations from three surface series discussed above, 1880-2008. Also shown are the same (pre 1900) multiproxies as in fig. B1. The simulations are for land only in the northern hemisphere whereas the surface data are global (including oceans). This difference presumably accounts for their slightly lower variability.

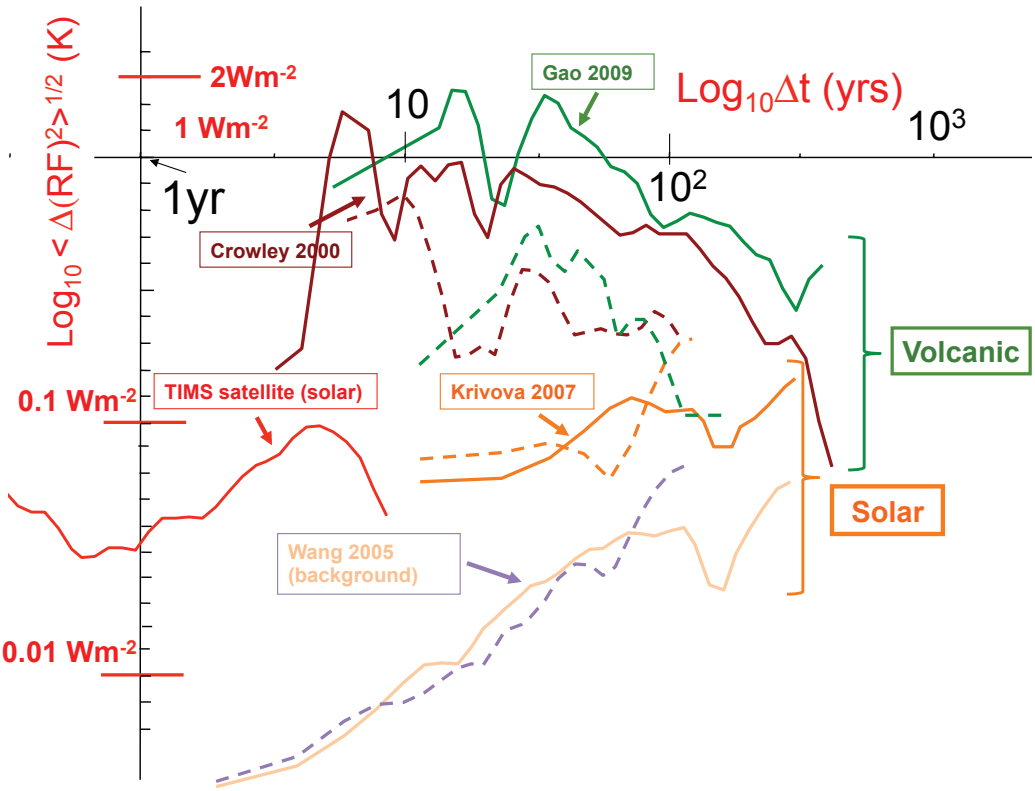


Fig. B3: The RMS radiative forcing fluctuations for the two volcanic series used in fig. B1, B2 (since 1500 [*Crowley*, 2000], [*Gao et al.*, 2008]) as well as the same from sunspot based solar reconstructions [*Wang et al.*, 2005], [*Krivova et al.*, 2007] (from 1610). The full lines are for the period up to 1900, the dashed lines for the period since 1880. One can see that the solar fluctuations are of nearly the same amplitude at all scales. In contrast, the volcanic forcings have decreased by a factor 2-3 in the recent period. For a more complete analysis of the fluctuations over the whole period, see [*Lovejoy and Schertzer*, 2012a].

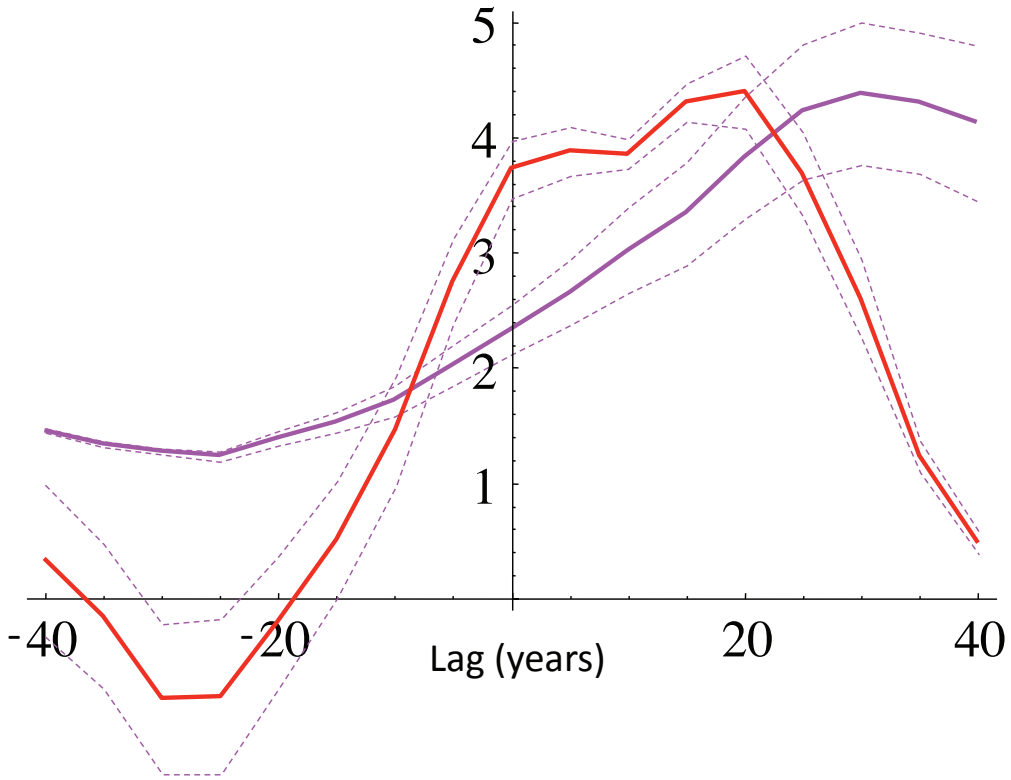


Fig. B4: The red curve is the 10x the cross correlation of the lagged $R_{FCO2}$ (from the $CO_2$ reconstruction of [*Frank et al.*, 2010]) and the global mean temperatures (averaged at 5 year resolution) with dashed lines indicating one standard deviation variations (as estimated from the three global mean temperature series), the curves were given a 1-2-1 smoother to bring out the overall variations. We can see that lags between zero and lag 20 years give nearly the same cross-correlation. However, the effective climate sensitivity to doubling $CO_2$ (purple) increases from 2.33±0.22 (zero lag) to 3.82±0.54 with a 20 year lag.

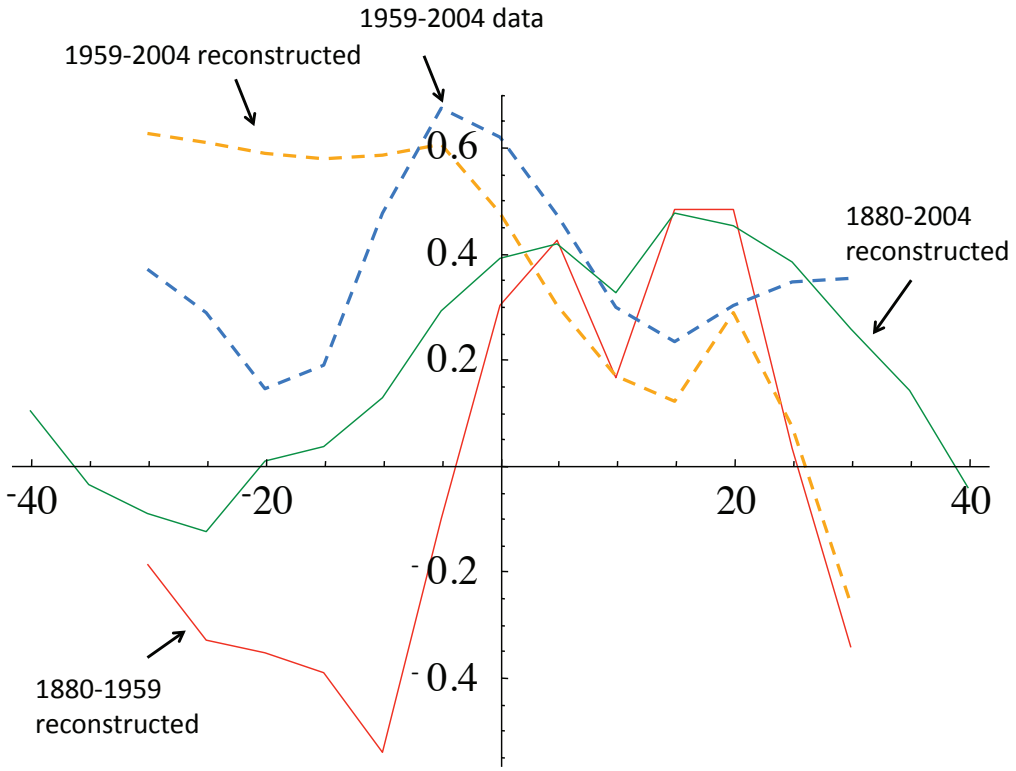


Fig. B5: This figure shows the cross correlation of $\log_2\rho_{CO2}$ and $T_{globe}$ (at 5 year resolution) for periods 1880-1959 and 1959-2004. In the recent period along with the $\rho_{CO2}$ reconstruction we use $\rho_{CO2}$ data (averaged from Mauna Loa and the South pole station). We see that there is agreement that for the recent period, the cross-correlation decreases after zero lag.

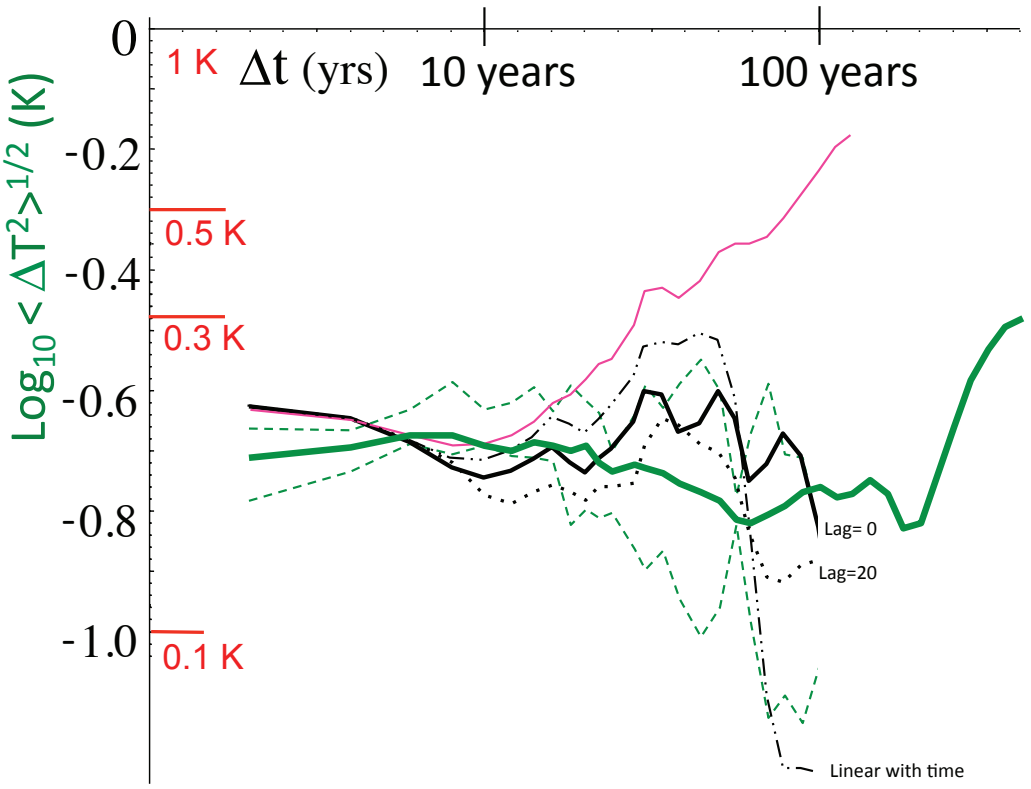


Fig. B6: This figure shows the top part of fig. 3 (but without the upward shift) and adds the RMS fluctuations for the 20 year lagged $\log_2\rho_{CO2}$ residuals (dotted, black) lines as well as the residuals of the linear temperature versus time regression (dot-dashed, black). Recall that the pink is the surface data 1880-2004 and the green are the multiproxies: thick green is the mean over 1500-1900, the dashed green are one standard deviation limits for the three 125 year epochs (1500-1624, 1625-1749, 1750-1874). Both the lagged and unlagged $\log_2\rho_{CO2}$ residuals are generally within the one standard deviation limits, although the 20 year lagged residuals are closer to the mean. The residuals of the $T_{globe}$ versus time regression are generally outside the one standard deviation limits for $\Delta t \approx >10$ years.

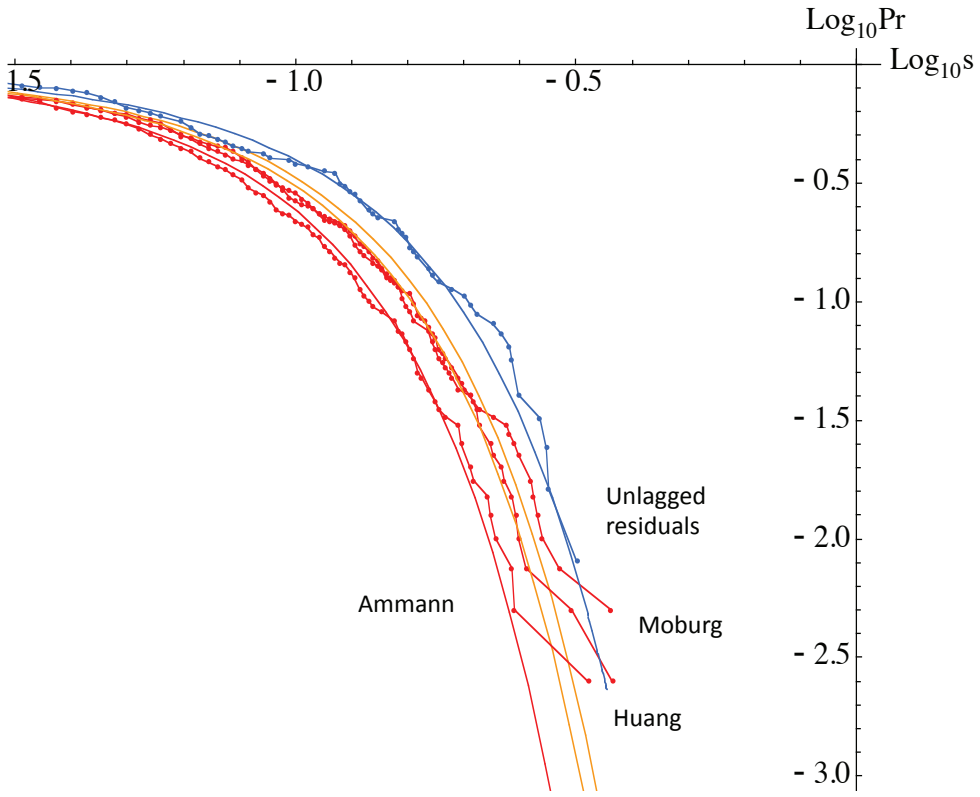


Fig. B7: The temperature differences for $\Delta t$ = 1 year for the three multiproxies (red, 1500-1900) compared with the (unlagged) residuals from fig. 1. The smooth curves are the Gaussians with the same standard deviations. We see that the multiproxies are quite close to each other – although with some small variations in amplitude - about 10% between each curve - but not much in shape. At this scale the residuals have slightly larger variability, although after $\Delta t \approx$ 10 - 20 years (see fig. 3), it falls within the epoch to epoch variations of the mean of the multiproxies.

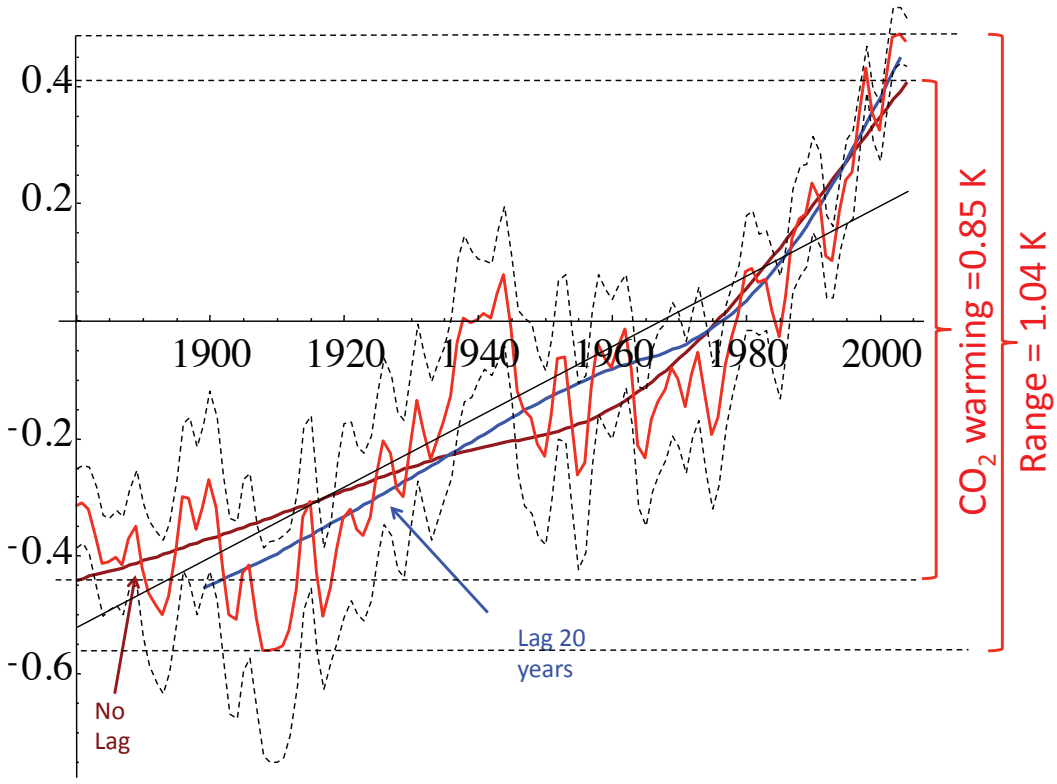


Fig. B8: The comparison of the mean global temperature series (red), one standard deviation limits (dashed, all from the three surface series discussed above), compared with the unlagged (brown, corresponding to fig. 1) and 20 year lagged (blue) estimates obtained from $\log_2 \rho_{CO2}$ versus $T_{globe}$ regressions as discussed in the text. Also shown in the regression of the latter with time (straight line) as well the overall estimates $\Delta T_{anth}$ =0.85 for the unlagged relation and the overall range $\Delta T_{\text{globe,range}}$ which presumably bounds $\Delta T_{anth}$.

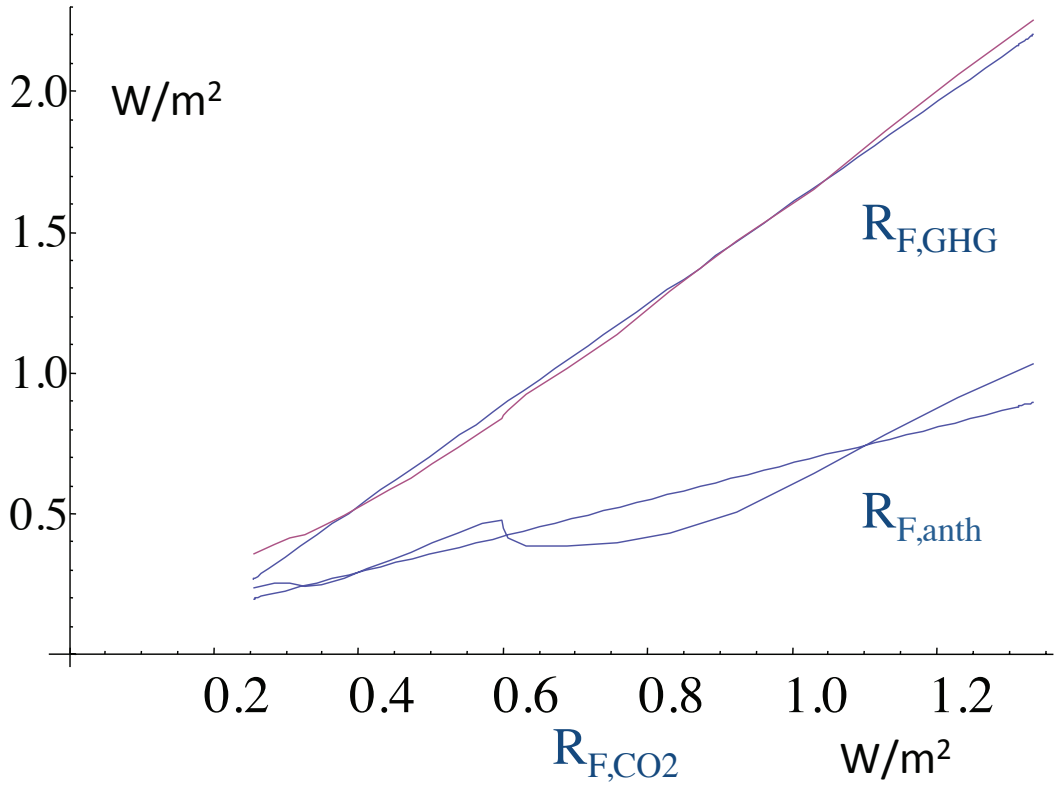


Fig. B9: Over the period 1880-1995, the relationship between the radiative forcing of CO2 ($R_{F,\,CO2}$), the radiative forcing of all the long lived Greenhouse Gases (including $CO_2$: $R_{F,\,GHG}$) and the total radiative forcing of all the anthropogenic emission including aerosols; data from [*Myhre et al.*, 2001]. The regression lines have equations $R_{F,GHG} = -0.190 \pm 0.019 + (1.793 \pm 0.027) R_{F,CO_2}$ and $R_{F,anth} = 0.034 \pm 0.033 + (0.645 \pm 0.048) R_{F,CO_2}$.


## Acknowledgements:

I thank R. Pielke sr. for useful comments. This work was unfunded; there were no conflicts of interest.


## References


Ammann, C. M., Joos, F., D. S. Schimel, R. Otto-Bliesner, B. L., and A. Tomas (2007), Solar Influence on Climate during the Past Millennium: Results from Transient Simulations with the NCAR Climate System, *Proc. of the Nat. Acad. of Sci. USA*, *104, (10)*, 3713-3718.

Bauer, S., and E. Menon (2012), Aerosol direct, indirect, semidirect, and surface albedo effects from sector contributions based on the IPCC AR5 emissions for preindustrial and present-day conditions, *J. Geophys. Resear. (Atmos.)*, *117* doi: 10.1029/2011JD016816.

Brohan, P., J. J. Kennedy, I. Harris, S. F. B. Tett, and P. D. Jones (2006), Uncertainty estimates in regional and global observed temperature changes: a new dataset from 1850, *J. Geophysical Research*, *111*, D12106 doi: doi:10.1029/2005JD006548

Crowley, T. J. (2000), Causes of Climate Change Over the Past 1000 Years, *Science*, *289*, 270 doi: 10.1126/science.289.5477.270.

Frank, D. C., J. Esper, C. C. Raible, U. Buntgen, V. Trouet, B. Stocker, and F. Joos (2010), Ensemble reconstruction constraints on the global carbon cycle sensitivity to climate, *Nature*, *463 (28)* doi: doi:10.1038/nature08769.

Gao, C. G., A. Robock, and C. Ammann (2008), Volcanic forcing of climate over the past 1500 years: and improved ice core-based index for climate models, *J. Geophys. Res.*, *113*, D23111 doi: 10.1029/2008JD010239.

Hansen, J., R. Ruedy, M. Sato, and K. Lo (2010), Global surface temperature change, *Rev. Geophys.*, *48*, RG4004 doi: doi:10.1029/2010RG000345.

Hansen, J., et al. (2005), Earth's Energy Imbalance: Confirmation and Implications, *Science*, *308 no. 5727* 1431-1435 doi: 10.1126/science.1110252.

Huang, S. (2004), Merging Information from Different Resources for New Insights into Climate Change in the Past and Future, *Geophys.Res, Lett.* , *31*, L13205 doi: doi : 10.1029/2004 GL019781.

Knutti, R., T. F. Stocker, F. Joos, and G.-K. Plattner (2002), Constraints on radiative forcing and future climate change from observations and climate model ensembles, *Nature*, *416*, 719-723.

Krivova, N. A., L. Balmaceda, and S. K. Solanski (2007), Reconstruction of solar total irradiance since 1700 from the surface magnetic field flux, *Astron. and Astrophys*, *467*, 335-346 doi: 10.1051/0004-6361:20066725.

Lean, J. L. (2000), Evolution of the Sun's Spectral Irradiance Since the Maunder Minimum, *Geophys. Research Lett.*, *27*, 2425-2428.

Ljundqvist, F. C. (2010), A new reconstruction of temperature variability in the extra - tropical Northern Hemisphere during the last two millennia, *Geografiska Annaler: Physical Geography*, *92 A*(3), 339 - 351 doi: DOI : 10.1111/j .1468 - 0459.2010 .00399.x.

Lovejoy, S. (2013), What is climate?, *EOS*, *94, (1), 1 January*, p1-2.

Lovejoy, S., and D. Schertzer (1986), Scale invariance in climatological temperatures and the spectral plateau, *Annales Geophysicae*, *4B*, 401-410.

Lovejoy, S., and D. Schertzer (2012a), Stochastic and scaling climate sensitivities: solar, volcanic and orbital forcings, *Geophys. Res. Lett.* , *39*, L11702 doi: doi:10.1029/2012GL051871.

Lovejoy, S., and D. Schertzer (2012b), Haar wavelets, fluctuations and structure functions: convenient choices for geophysics, *Nonlinear Proc. Geophys.* , *19*, 1-14 doi: 10.5194/npg-19-1-2012.

Lovejoy, S., and D. Schertzer (2012c), Low frequency weather and the emergence of the Climate, in *Extreme Events and Natural Hazards: The Complexity Perspective*, edited by A. S. Sharma, A. Bunde, D. Baker and V. P. Dimri, pp. 231-254, AGU monographs.

Lovejoy, S., and D. Schertzer (2013a), The climate is not what you expect, *Bull. Amer. Meteor. Soc.*, *(in press)*.

Lovejoy, S., and D. Schertzer (2013b), *The Weather and Climate: Emergent Laws and Multifractal Cascades*, 480 pp., Cambridge University Press, Cambridge.

Lovejoy, S., D. Schertzer, and D. Varon (2012a), Do GCM's predict the climate…. or macroweather?, *Earth Syst. Dynam. Discuss.*, *3,* , 1259-1286 doi: 10.5194/esdd-3-1259-2012.

Lovejoy, S., D. Schertzer, and D. Varon (2012b), Response to R. Betts: Interactive comment on "Do GCM's predict the climate... or macroweather?" *Earth Syst. Dynam. Discuss.*, *3*, C778–C783.

Lovejoy, S., D. Scherter, and D. Varon (2013), How scaling fluctuation analyses change our view of the climate and its models (Reply to R. Pielke sr.: Interactive comment on "Do GCM's predict the climate... or macroweather?" by S. Lovejoy et al.), *Earth Syst. Dynam. Discuss.*, *3*, C1–C12.

Lyman, J. M., S. A. Good, V. V. Gouretski, M. Ishii, G. C. Johnson, M. D. Palmer, D. M. Smith, and J. K. Willis (2010), Robust warming of the global upper ocean, *Nature*, *465*, 334–337 doi: 10.1038/nature09043.

Moberg, A., D. M. Sonnechkin, K. Holmgren, and N. M. Datsenko (2005), Highly variable Northern Hemisphere temperatures reconstructed from low- and high - resolution proxy data, *Nature*, *433*(7026), 613-617.

Myhre, G. (2009), Consistency Between Satellite-Derived and Modeled Estimates of the Direct Aerosol Effect, , *Science*, *325 (5937)* 187-190 doi: DOI: 10.1126/science.1174461.

Myhre, G., A. Myhre, and F. Stordal (2001), Historical evolution of radiative forcing of climate, *Atmos. Environ.* , *35*, 2361-2373.

Peng, C.-K., S. V. Buldyrev, S. Havlin, M. Simons, H. E. Stanley, and A. L. Goldberger (1994), Mosaic organisation of DNA nucleotides, *Phys. Rev. E*, *49*, 1685-1689.

Peterson, T. C., and R. S. Vose (1997), An overview of the Global Historical Climatology Network temperature database, *Bull. Amer. Meteorol. Soc.*, *78*, 2837-2849 doi: doi:10.1175/1520-0477.

Rayner, N. A., P. Brohan, D. E. Parker, C. K. Folland, J. J. Kennedy, M. Vanicek, T. Ansell, and S. F. B. Tett (2006), Improved analyses of changes and uncertainties in marine temperature measured in situ since the mid-nineteenth century: the HadSST2 dataset. , *J. Climate*, *19*, 446-469.

Schertzer, D., and S. Lovejoy (1987), Physical modeling and Analysis of Rain and Clouds by Anisotropic Scaling of Multiplicative Processes, *Journal of Geophysical Research*, *92*, 9693-9714.

Shapiro, A. I., W. Schmutz, E. Rozanov, M. Schoell, M. Haberreiter, A. V. Shapiro, and S. Nyeki (2011), A new approach to long-term reconstruction of the solar irradiance leads to large historical solar forcing, *Astronomy & Astrophysics*, *529*, A67 doi: doi.org/10.1051/0004-6361/201016173.

Smith, T. M., R. W. Reynolds, T. C. Peterson, and J. Lawrimore (2008), Improvements to NOAA's Historical Merged Land-Ocean Surface Temperature Analysis (1880-2006), *J. Climate*, *21*, 2283-2293.

Steinhilber, F., J. Beer, and C. Frohlich (2009), Total solar irradiance during the Holocene, *Geophys. Res. Lett.*, *36*, L19704 doi: 10.1029/2009GL040142.

Van Aardenne, J. A., F. J. Dentener, J. G. J. Olivier, C. G. M. Klein Goldewijk, and J. Lelieveld (2001), A 1 x 1 degree resolution dataset of historical anthropogenic trace gas emissions for the period 1890 - 1990, *Global Biogeochemical Cycles*, *15 (4)*, 909 - 928.

van Oldenborgh, G. J., F. J. Doblas-Reyes, B. Wouters, and W. Hazeleger (2012), Decadal prediction skill in a multi-model ensemble, *Clim. Dyn.* doi: 0.1007/s00382-012-1313-4.

Wang, Y.-M., J. L. Lean, and N. R. J. Sheeley (2005), Modeling the Sun's magnetic field and irradiance since 1713, *Astrophys J.* , *625*, 522–538.

Wigley, T. M. L., P. D. Jones, and S. C. B. Raper ( 1997), The observed global warming record: What does it tell us?, *Proc. Natl. Acad. Sci. USA*, *94*, 8314–8320.